Effect of Fiber Tracts and Depolarized Brain Volume on Resting Motor Thresholds During Transcranial Magnetic Stimulation

Neil Mittal[1], Connor Lewis[1], Yeajin Cho[1], Carrie L. Peterson[1], and Ravi L. Hadimani[1,2]

[1]Department of Biomedical Engineering, Virginia Commonwealth University, Richmond, VA 23220 USA
[2]Department of Mechanical and Nuclear Engineering, Virginia Commonwealth University, Richmond, VA 23220 USA

Transcranial magnetic stimulation (TMS) is a treatment procedure for some neuropsychiatric disorders, and it has been used for brain mapping, as well as diagnosis and treatment of neuromuscular dysfunctions. There is a disconnect between TMS modeling and clinical data: several groups have reported the simulated induced electric field and measured resting motor threshold (RMT) with inconsistent results in the relationship between RMT and brain scalp distance. This necessitates the use of simulation parameters that further account for individual differences in neuroanatomy. We recruited ten healthy subjects and obtained empirical RMT, magnetic resonance imaging (MRI), and diffusion tensor imaging (DTI). We developed anatomically accurate brain models from MRI and simulated TMS to determine the percent depolarized volume of gray matter (DVG) from TMS-induced electric fields. Corticospinal fiber tracts were extracted from the primary motor cortex from DTI to obtain fiber tract surface areas (FTSAs) for each participant. Linear mixed-effects models were used to evaluate the effect of DVG and FTSA on RMT. We report that DVG correlates with RMT when accounting for corticospinal FTSA.

***Index Terms*—Magnetic resonance imaging, motor evoked potentials, neuroplasticity, resting motor threshold (RMT), transcranial magnetic stimulation (TMS).**

ABBREVIATIONS

B	Magnetic field.
DTI	Diffusion tensor imaging.
DVG	Depolarized volume of gray matter.
E	Electric field.
MRI	Magnetic resonance imaging.
RMT	Resting motor threshold.
TMS	Transcranial magnetic stimulation.

I. INTRODUCTION

FINITE element modeling simulations of TMS using complex head models and coils have been used to better understand neuromodulation strategies. TMS is a promising neuromodulation paradigm for brain mapping, diagnostics, and treatment of neurological and psychiatric disorders [1]–[5]. However, it is limited by high intra- and inter-subject variability in its effects [1], [6]–[14]. The methods of modeling derived from magnetic resonance imaging (MRI) have been used with TMS to tailor stimulation protocols [1], and to connect individual neuroanatomy to variations in response to measurement of the brain scalp distance, including a study by Lotze *et al.* [17], which found that brain scalp distance explained some disparity between functional MRI (fMRI) and TMS brain mapping [15], [16]. Brain scalp distance, however, as a single dimensional measurement, fails to account for the composition of tissue between the scalp and cortex. Induced electric field strength from the magnetic field generated by the TMS coil, however, is a 3-D parameter and accounts for greater complexity of tissue organization [18].

Individual differences in neuroanatomy will influence TMS response as the induced electric field is dependent on the brain morphology, and communication along a pathway is dependent on the fiber tracts leading from the cortex to the spine [8], [15], [18]–[23]. TMS responses from the motor cortex can be characterized by the RMT, which has two definitions. From the perspective of neuron depolarization, RMT is the stimulation intensity in percentage of maximum stimulator output required to induce cortical electric field strength of at least 100 V/m [24]. From a motor response perspective, in a clinical setting, RMT is defined as the stimulus intensity, also in percentage of maximum stimulator output, that elicits a motor evoked potential of at least 50 mV in at least five out of ten consecutive stimuli [25], [26]. These motor evoked potentials are variable between individuals, and physical differences between individuals can affect both motor evoked potential amplitude and interpretation [27]. These definitions are linked because electric field strength of at least 100 V/m is the threshold of consistent depolarization of neurons, which would lead to the motor evoked potentials. However, the current simulation work has not investigated the simulated electric field strength and RMT in the context of individual-level anatomical variation while considering inter-subject fiber tracts for differences in corticospinal communication, and simultaneously compared to the empirical response to TMS.

The motor cortex and corticospinal tract's response to TMS is of particular interest in motor rehabilitation. Brain stimulation can prime the corticospinal system prior to motor training, and thereby improve motor relearning [28]–[30];

Manuscript received 29 October 2021; revised 4 January 2022; accepted 25 January 2022. Date of publication 31 January 2022; date of current version 26 July 2022. Corresponding authors: N. Mittal and R. L. Hadimani (e-mail: neil.mittal@gmail.com; rhadimani@vcu.edu).

This work involved human subjects or animals in its research. Approval of all ethical and experimental procedures and protocols was granted by the IRB through Virginia Commonwealth University IRB under Application No. HM20018505 and ClinicalTrials Registration through clinicaltrials.gov under Application No. NCT04586387.

Color versions of one or more figures in this article are available at https://doi.org/10.1109/TMAG.2022.3148214.

Digital Object Identifier 10.1109/TMAG.2022.3148214

This work is licensed under a Creative Commons Attribution-NonCommercial-NoDerivatives 4.0 License.
For more information, see https://creativecommons.org/licenses/by-nc-nd/4.0/

this has been found in healthy individuals and those with motor impairment, where repetitive TMS applied to arm or leg cortical representations of the primary motor cortex increased corticomotor excitability, voluntary motor control, and motor learning [9], [22], [31], [32].

The purpose of this study was to investigate the effect of neuroanatomy on the response to TMS. Several studies have investigated the relationship between brain scalp distance and TMS responses with varying conclusions [15], [27], [33]–[35]. In this study, we have investigated the dependence of RMT on neuroanatomy including fiber tracts, which is related to functional connectivity in the motor pathway network. RMT was recorded from human subjects to establish a TMS motor response, while simulated TMS was applied to individualized, anatomically accurate head models derived from MRI of the same human participants. Electric field strength and head models were used to calculate the percent of DVG, to incorporate cortical interconnectivity into the anatomical metric of electric field strength. Fiber tractography was carried out to calculate the fiber tract surface area (FTSA), representing the neural communication architecture along the motor pathway of interest. DVG and FTSA were compared to the empirically collected RMT. We hypothesized that RMT would negatively correlate with DVG, indicating greater TMS response with more brain volume depolarization. Furthermore, we hypothesized that the relationship between DVG and RMT would depend on the FTSA.

II. Methods

A. Participants and Empirical TMS Sessions

Ten individuals (seven females, three males, 23.5 ± 5 years) participated after screening to ensure safety of the TMS and MRI protocols and providing informed consent. Eligible participants were between the ages of 18 and 65 years old. Severe medical illness and sequelae, existing infection, cardiovascular disease, significant osteoporosis, metal implanted devices, personal or family history of seizure activity, and any acute or current history of neuromuscular or motor dysfunction were exclusionary. Participants underwent TMS sessions targeting the motor hotspot of the first dorsal interosseous as described by Mittal *et al.* [6]. Each participant had two RMT measurements in their session, to account for intra-subject variability (see Section II-C). This study was approved by the Virginia Commonwealth University Institutional Review Board (Study ID: HM20018505), Clinical Trial Registration: ClinicalTrials.gov: NCT04586387 [50].

B. MRI-Derived TMS Simulations and Modeled Parameters

Structural T1- and T2-weighted images and whole brain diffusion-weighted images were acquired for head model generation and fiber tractography from diffusion tensor imaging (DTI), respectively.

Extracted T1- and T2-weighted images from all the subjects passed a SimNIBS pipeline (SimNIBS Developers 2019, v2.0.1) [15], [33] to create individual segments. Abnormalities were smoothed using Meshmixer (AutoDesk, Inc., v11.2.37) (Fig. 1).

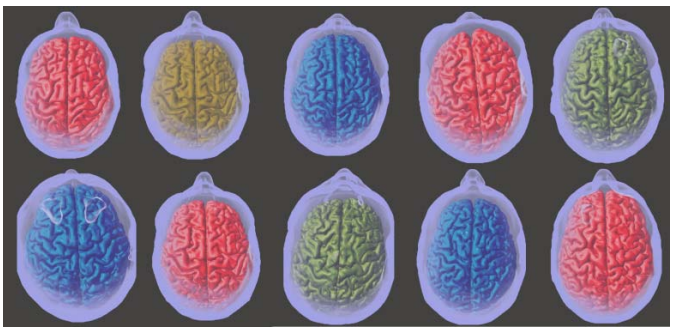

Fig. 1. Anatomical variation. Head models from each participant are visualized (participant ID. 1–10, from top left, across, then to bottom left and across). Each head model is distinct and made to the MRI of an individual participant.

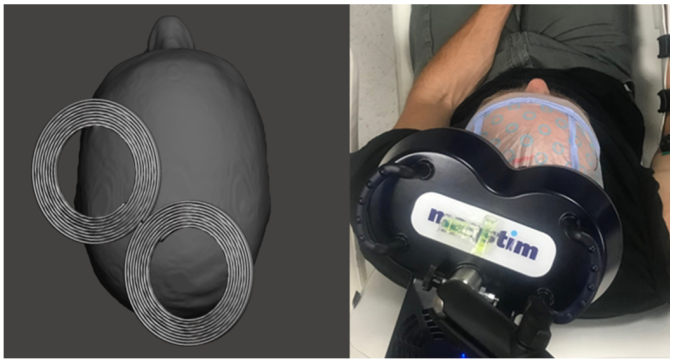

Fig. 2. Coil positioning. Left: The simulated coil is placed to induce a monophasic anterior-to-posterior current on the cortex, maximally over the region of upper motor control in the primary motor cortex. Right: TMS session setup for coil placement after adjustments to find the optimal empirical point of target.

Sim4Life finite element analysis software (Zurich Med Tech, v6.2.1.4972) was used to compute magnetic field, B, and induced electric field, E, on the generated head models from peak intensity stimulation of the primary motor cortex [15], [16], [18], [36]. The simulated coil matched dimensions of the Magstim 70 mm figure-of-eight coil [37], oriented to match the empirical setup (Fig. 2), targeting the precentral gyrus posterior to the superior frontal sulcus, within the "knob" as defined by Yousry *et al.* [38].

The stimulation current strength was set to 5000 A, corresponding to 100% maximum stimulator output, at 2500 Hz [18] and the segments of the head model and air were assigned material properties based on the IT'IS LF database (IT'IS Foundation, v4.0).

Electrical conductivity of gray matter, white matter, and cerebrospinal fluid were 0.24, 0.27, and 1.78 S/m, respectively. The relative permeability of all the materials (to air) was 1. The magnetic stimulation was calculated based on stimulator and model material parameters (Fig. 3). Induced electric field strength at the surface of the cortex, specifically of the gray matter segment, was interpolated (Fig. 4), and the gray matter electrical field vectors for each voxel were extracted [18]. The root mean square was calculated to find the electric field strength at each individual voxel for the gray matter. DVG

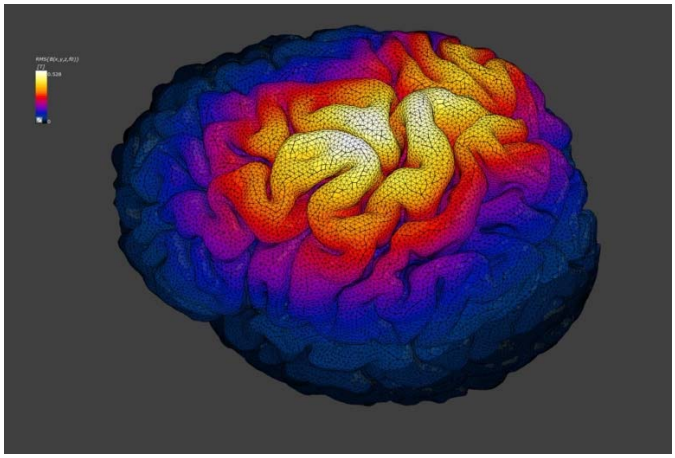

Fig. 3. Simulated magnetic field on cortex (sagittal plane). The magnetic field generated by the TMS coil was generated within the head model. Magnetic field strength (B-field) was determined based on the coil parameters, positioning, and material mediums in the head models. Maximal stimulation was located over the upper limb motor control region of the primary motor cortex. White is maximum B-field, 0.528 T, to dark blue, 0 T.

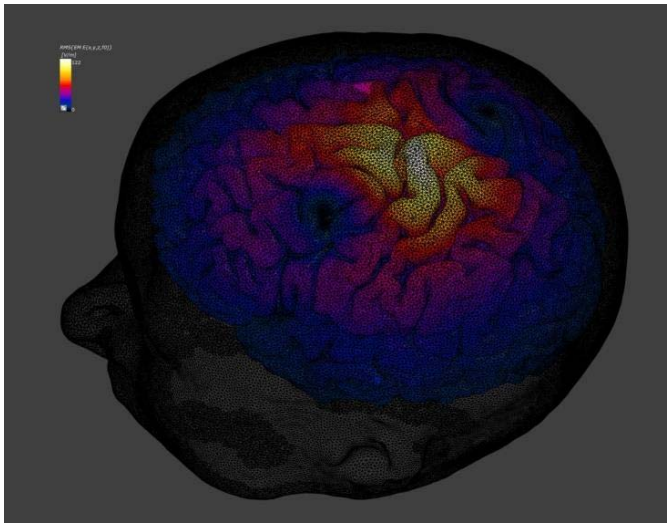

Fig. 4. Induced electric field strength on cortex (sagittal plane). Finite element simulations of magnetic stimulation delivered to individual head models were performed to calculate electric field strength based on the magnetic field. Maximal stimulation is located over the upper limb motor control region of the primary motor cortex. White is maximum electric field strength, 122 V/m. to dark blue, 0 V/m.

was found by calculating the percent of voxels above the threshold of 100 V/m using MATLAB (MathWorks, MATLAB v 9.7.0.1190202).

Fiber tracts were extracted from DTI using DSI Studio (Feh, DSI Studio, 2020) based on the anatomical landmarks (superior frontal sulcus, precentral sulcus, central sulcus, and precentral gyrus) to the "knob" of the primary motor cortex [38]. A 6 mm diameter region of interest seeded extraction of fibers [39] (Fig. 5). Fiber coordinates were then imported into SolidWorks (BIOVIA, Dassault Systèmes, SolidWorks, SP3.0, San Diego: Dassault Systèmes, 2017) to calculate the FTSA for each model's fiber tract.

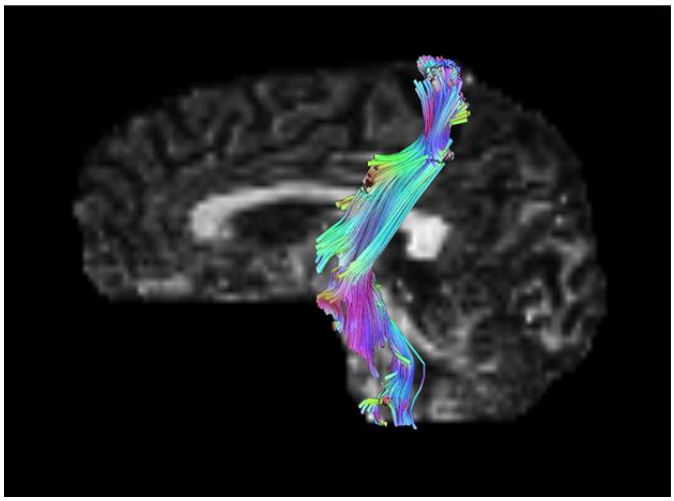

Fig. 5. Fiber tractography. Corticospinal fiber tracts were extracted from DTI beginning from a region of interest that encompassed upper limb motor control in the primary motor cortex.

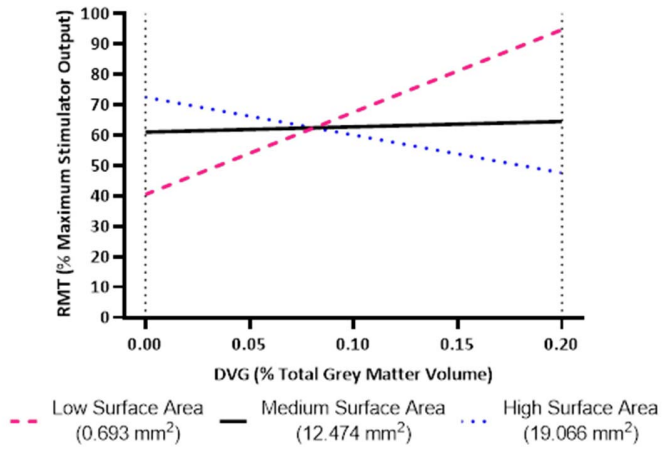

Fig. 6. Effect of DVG on RMT. RMT was found to correlate with DVG when accounting for fiber tract geometry in the form of FTSA. Larger tracts exhibited the expected negative correlation between RMT and DVG given the equation: $\mathrm{RMT}_{\mathrm{V/m}} = -124.52 * \mathrm{DVG}_{\%\mathrm{brain\ volume}} + 72.45$.

C. Statistical Analysis

Spearman's correlation tested for associations between either DVG or FTSA and RMT. Linear mixed-effects models tested for associations between DVG and FTSA and their effects on RMT in R (The R Foundation, v3.4.3) [40], [41]. Participants were included in the statistical model due to having two measurements for each, as a random effect to account for intra-session, intra-subject variability between multiple RMT measurements in a single session and from a single individual.

III. Results

A. Magnetic Fields, B, and Induced Electric Fields, E

Magnetic fields, B, and electric fields, E, were calculated in all the regions of the brain for the ten subjects. The peak fields in all subjects were determined below the figure-of-eight

TABLE I
SIMULATION PARAMETERS FOR EACH PARTICIPANT

Participant	B[a]	E[b]	DVG[c]	FTSA[d]
01	0.528	122	0.18	12.5
02	0.412	90.5	0.00	2.7
03	0.442	112	0.07	18.2
04	0.435	122	0.11	19.1
05	0.519	147	0.27	11.0
06	0.415	87.8	0.00	11.0
07	0.425	92.2	0.00	0.7
08	0.512	110	0.26	19.9
09	0.471	116	0.12	15.6
10	0.501	113	0.11	14.2
Mean ± SD	0.4660 ± 0.045	111.3 ± 17	0.110 ± 0.00	12.48 ± 6.5

a) B: magnetic (B) field strength, presented in T; b) E: electric (E) field strength, presented in V/m; c) DVG: depolarized volume of grey matter, presented as percent total volume grey matter; d) FTSA: fiber tract surface area (functional connectivity), presented in mm^2.

TABLE II
RMT FOR EACH PARTICIPANT

Participant	Age	FDI RMT[a]	
01	21	46	49
02	24	41	41
03	19	68	55
04	20	64	64
05	23	72	78
06	19	70	50
07	32	43	43
08	26	41	33
09	29	54	51
10	27	70	68
Mean ± SD	23.5 ± 5	56.9 ± 13	53.2 ± 14

a) FDI RMT: resting motor threshold of the first dorsal interosseus, presented as percent of maximum stimulator output. Both values were taken during the same session, spaced approximately one hour apart.

coil on the upper limb control area of the motor cortex which we intended to target. Table I shows the variation of B- and E-fields of all ten subjects. These values are similar to the reported B- and E-field values reported in the literature by other researchers [37], [42]–[44].

B. TMS Response (RMT)

Table II shows the first dorsal interosseous RMT of ten subjects along with their age and both RMTs for each session. There was no correlation between RMT and DVG alone ($p = 0.17$). There was no correlation between RMT and FTSA alone ($p = 0.9$).

C. Effect of DVG on FTSA on RMT

DVG and FTSA values are presented in Table I. There was no association between RMT and DVG alone ($p = 0.17$). There was no association between RMT and FTSA alone ($p = 0.9$).

D. Association Between DVG and FTSA

A linear mixed-effects model including the interactions between DVG and FTSA revealed an association between RMT and DVG ($p < 0.001$). RMT negatively correlated with DVG, but only at high FTSA. The correlation became less negative as FTSA decreased, until a positive correlation was observed at the lowest FTSA range. These relationships can be seen in Fig. 6.

DVG and FTSA were positively correlated ($p = 0.013$).

IV. DISCUSSION

The objective of this preliminary study was to investigate the association between modeled DVG above a threshold electric field and empirical TMS responsiveness (i.e., RMT). The secondary objective was to determine the influence of fiber tract geometry (FTSA) on the empirical TMS responsiveness to brain depolarization. The hypothesis that RMT would correlate negatively with DVG was partially supported; this relationship was found with a negative correlation between RMT and DVG, but only when accounting for fiber tract geometry, with larger fiber tracts (high FTSA).

The interaction between DVG and fiber tract geometry suggests that the expected relationship between brain depolarization and TMS evoked motor response is dependent on the connectivity within the cortex and overall neuroanatomy. Previous studies also support that the relationship between brain depolarization and TMS evoked motor response, which is dependent on the connectivity within the cortex and neuroanatomy. Rossi *et al.* [45] discussed age-related influences on TMS intensity variation between individuals, with neuroanatomical differences between children and older individuals being one driver in the intensity variation. Cantone *et al.* [27] showed that individual physiological differences affect the amplitudes of motor evoked potentials elicited by TMS, further highlighting the impact of individual neuroanatomy. TMS studies paired with electroencephalography have shown that induced activity spreads along motor networks [46], and cortical connectivity and hemodynamics can be modulated by repetitive TMS paradigms [47], i.e., it would expect more depolarized brain results in a motor response with less required stimulation as the brain is more sensitive to stimulation as a whole. This did occur in the present study in the presence of higher FTSA, as FTSA was a metric of cortical connectivity. High DVG and low RMT would be expected in a more responsive anatomical architecture due to greater connectivity, while larger fiber tracts would be expected to effectively transmit this from the cortex as greater cortical connectivity promotes TMS response [46]. The association between DVG and FTSA supports that both parameters would indicate aspects of neural connectivity, DVG electromagnetically, and FTSA synaptically. Thus, when both the DVG and FTSA are large, RMT is decreased. RMT depends on DVG in a predictively linear fashion if FTSA is considered. However, when fiber tracts are smaller, the relationship between brain depolarization and motor output requires further investigation.

V. CONCLUSION

This was a preliminary study with some limitations, and future work is needed. This study is limited by a small sample size that included no subjects with brain disorders. The effects

of neuropathology on the relationships investigated would be essential to ascertain before developing treatment paradigms and future studies should include greater sample sizes and pathologically diverse groups to investigate the influence of neurological disorder on these relationships. However, the addition of diagnostic variables to a proof-of-concept study would make it difficult to characterize the interaction of these parameters at baseline. Furthermore, electric field strength is a time-varying parameter, but was evaluated using a quasi-static solver for finite element analysis, due to computational limitations. The analyses presented are associative only, rather than causational. Future work should investigate causal mechanisms and further clarify the directionality of the uncovered associations. Last, DTI was used for proof of concept, but future study with more sophisticated methods, such as neurite orientation dispersion and density imaging [48] or fixel-based analysis [49], would allow for greater insights of effects of individual variability in neuroanatomy.

Our results show that the effects of TMS are governed by cortical organization due to anatomy and fiber tract geometry. Further investigation is needed to understand the mechanistic drivers of the relationship between depolarized brain volume and RMT at different fiber tract sizes.

ACKNOWLEDGMENT

This work was supported in part by the Virginia Commonwealth University's Center for Rehabilitation Science and Engineering and Dean's Undergraduate Research Initiative and in part by the Commonwealth Cyber Initiative under Grant FP00010500.

The authors would like to thank Bhushan Thakkar, Cooper Hodges, Brent Nevadomski, Abigail Andrade, and Keith Li for their assistance with data collection and processing.

REFERENCES

[1] A. A. Herrold *et al.*, "Customizing TMS applications in traumatic brain injury using neuroimaging," *J. Head Trauma Rehabil.*, vol. 35, no. 6, pp. 401–411, Nov. 2020, doi: 10.1097/HTR.0000000000000627.

[2] J. Korzhova *et al.*, "High-frequency repetitive transcranial magnetic stimulation and intermittent theta-burst stimulation for spasticity management in secondary progressive multiple sclerosis," *Eur. J. Neurol.*, vol. 26, no. 4, p. 680-e44, Apr. 2019, doi: 10.1111/ENE.13877.

[3] A. E. Pink, C. Williams, N. Alderman, and M. Stoffels, "The use of repetitive transcranial magnetic stimulation (rTMS) following traumatic brain injury (TBI): A scoping review," *Neuropsychol. Rehabil.*, vol. 31, no. 3, pp. 479–505, Mar. 2021, doi: 10.1080/09602011.2019.1706585.

[4] P. A. Spagnolo, J. Parker, S. Horovitz, and M. Hallett, "Corticolimbic modulation via intermittent theta burst stimulation as a novel treatment for functional movement disorder: A proof-of-concept study," *Brain Sci.*, vol. 11, no. 6, p. 791, Jun. 2021, doi: 10.3390/BRAINSCI11060791.

[5] W. Klomjai, R. Katz, and A. Lackmy-Vallée, "Basic principles of transcranial magnetic stimulation (TMS) and repetitive TMS (rTMS)," *Ann. Phys. Rehabil. Med.*, vol. 58, no. 4, pp. 208–213, Sep. 2015, doi: 10.1016/J.REHAB.2015.05.005.

[6] N. Mittal, B. C. Majdic, A. P. Sima, and C. L. Peterson, "The effect of intermittent theta burst stimulation on corticomotor excitability of the biceps brachii in nonimpaired individuals," *Neurosci. Lett.*, vol. 764, Nov. 2021, Art. no. 136220, doi: 10.1016/J.NEULET.2021.136220.

[7] A. Guerra, V. López-Alonso, B. Cheeran, and A. Suppa, "Variability in non-invasive brain stimulation studies: Reasons and results," *Neurosci. Lett.*, vol. 719, Feb. 2020, Art. no. 133330, doi: 10.1016/j.neulet.2017.12.058.

[8] M. Hamada, N. Murase, A. Hasan, M. Balaratnam, and J. C. Rothwell, "The role of interneuron networks in driving human motor cortical plasticity," *Cerebral Cortex*, vol. 23, no. 7, pp. 1593–1605, Jul. 2013, doi: 10.1093/cercor/bhs147.

[9] M. R. Hinder *et al.*, "Inter- and intra-individual variability following intermittent theta burst stimulation: Implications for rehabilitation and recovery," *Brain Stimulation*, vol. 7, no. 3, pp. 365–371, May 2014, doi: 10.1016/J.BRS.2014.01.004.

[10] Y. Z. Huang *et al.*, "Plasticity induced by non-invasive transcranial brain stimulation: A position paper," *Clin. Neurophysiol.*, vol. 128, pp. 2318–2329, Nov. 2017, doi: 10.1016/j.clinph.2017.09.007.

[11] V. López-Alonso, B. Cheeran, D. Río-Rodríguez, and M. Fernández-del-Olmo, "Inter-individual variability in response to non-invasive brain stimulation paradigms," *Brain Stimulation*, vol. 7, no. 3, pp. 372–380, May 2014, doi: 10.1016/j.brs.2014.02.004.

[12] R. Perellón-Alfonso *et al.*, "Similar effect of intermittent theta burst and sham stimulation on corticospinal excitability: A 5-day repeated sessions study," *Eur. J. Neurosci.*, vol. 48, no. 4, pp. 1990–2000, Aug. 2018, doi: 10.1111/ejn.14077.

[13] C. Nettekoven *et al.*, "Inter-individual variability in cortical excitability and motor network connectivity following multiple blocks of rTMS," *NeuroImage*, vol. 118, pp. 18–209, Sep. 2015, doi: 10.1016/j.neuroimage.2015.06.004.

[14] N. Sollmann *et al.*, "Clinical factors underlying the inter-individual variability of the resting motor threshold in navigated transcranial magnetic stimulation motor mapping," *Brain Topography*, vol. 30, no. 1, pp. 98–121, Nov. 2016, doi: 10.1007/S10548-016-0536-9.

[15] E. G. Lee *et al.*, "Investigational effect of brain-scalp distance on the efficacy of transcranial magnetic stimulation treatment in depression," *IEEE Trans. Magn.*, vol. 52, no. 7, pp. 1–4, Jul. 2016, doi: 10.1109/TMAG.2015.2514158.

[16] L. J. Crowther, R. L. Hadimani, and D. C. Jiles, "Effect of anatomical brain development on induced electric fields during transcranial magnetic stimulation," *IEEE Trans. Magn.*, vol. 50, no. 11, pp. 1–4, Nov. 2014, doi: 10.1109/TMAG.2014.2326819.

[17] M. Lotze, R. J. Kaethner, M. Erb, L. G. Cohen, W. Grodd, and H. Topka, "Comparison of representational maps using functional magnetic resonance imaging and transcranial magnetic stimulation," *Clin. Neurophysiol.*, vol. 114, no. 2, pp. 306–312, Feb. 2003, doi: 10.1016/S1388-2457(02)00380-2.

[18] F. Syeda, H. Magsood, E. G. Lee, A. A. El-Gendy, D. C. Jiles, and R. L. Hadimani, "Effect of anatomical variability in brain on transcranial magnetic stimulation treatment," *AIP Adv.*, vol. 7, no. 5, May 2017, Art. no. 056711, doi: 10.1063/1.4974981.

[19] V. Di Lazzaro *et al.*, "The physiological basis of the effects of intermittent theta burst stimulation of the human motor cortex," *J. Physiol.*, vol. 586, no. 16, pp. 9–3871, Aug. 2008, doi: 10.1113/jphysiol.2008.152736.

[20] Y. Z. Huang, M. J. Edwards, E. Rounis, K. P. Bhatia, and J. C. Rothwell, "Theta burst stimulation of the human motor cortex," *Neuron*, vol. 45, no. 2, pp. 201–206, Jan. 2005, doi: 10.1016/j.neuron.2004.12.033.

[21] L. Cárdenas-Morales *et al.*, "Network connectivity and individual responses to brain stimulation in the human motor system," *Cerebral Cortex*, vol. 24, no. 7, pp. 1697–1707, Jul. 2014, doi: 10.1093/cercor/bht023.

[22] Y.-H. Kim *et al.*, "Repetitive transcranial magnetic stimulation–induced corticomotor excitability and associated motor skill acquisition in chronic stroke," *Stroke*, vol. 37, no. 6, pp. 1471–1476, Jun. 2006, doi: 10.1161/01.STR.0000221233.55497.51.

[23] M. P. Malcolm, W. J. Triggs, K. E. Light, O. Shechtman, G. Khandekar, and L. J. G. Rothi, "Reliability of motor cortex transcranial magnetic stimulation in four muscle representations," *Clin. Neurophysiol.*, vol. 117, no. 5, pp. 1037–1046, May 2006, doi: 10.1016/j.clinph.2006.02.005.

[24] M. Lu and S. Ueno, "Comparison of the induced fields using different coil configurations during deep transcranial magnetic stimulation," *PLoS ONE*, vol. 12, no. 6, Jun. 2017, Art. no. e0178422, doi: 10.1371/journal.pone.0178422.

[25] J. J. Borckardt, Z. Nahas, J. Koola, and M. S. George, "Estimating resting motor thresholds in transcranial magnetic stimulation research and practice," *J. ECT*, vol. 22, no. 3, pp. 169–175, Sep. 2006, doi: 10.1097/01.yct.0000235923.52741.72.

[26] P. Rossini and A. Berardelli, "Guidelines of the IFCN (2nd Ed): Chapter 3.5 applications of magnetic cortical stimulation," *Clin. Neurophysiol.*, 1999. [Online]. Available: https://www.journals.elsevier.com/clinical-neurophysiology/view-for-free/guidelines-of-the-ifcn-2nd-ed-published-1999

[27] M. Cantone *et al.*, "Age, height, and sex on motor evoked potentials: Translational data from a large italian cohort in a clinical environment," *Frontiers Hum. Neurosci.*, vol. 13, p. 185, Feb. 2019, doi: 10.3389/FNHUM.2019.00185/BIBTEX.

[28] M. E. Stoykov and S. Madhavan, "Motor priming in neurorehabilitation," *J. Neurologic Phys. Therapy*, vol. 39, no. 1, pp. 33–42, Jan. 2015, doi: 10.1097/NPT.0000000000000065.

[29] J. Gomes-Osman, J. A. Tibbett, B. P. Poe, and E. C. Field-Fote, "Priming for improved hand strength in persons with chronic tetraplegia: A comparison of priming-augmented functional task practice, priming alone, and conventional exercise training," *Frontiers Neurol.*, vol. 7, Jan. 2017, doi: 10.3389/fneur.2016.00242.

[30] S. J. Ackerley, W. D. Byblow, P. A. Barber, H. MacDonald, A. McIntyre-Robinson, and C. M. Stinear, "Primed physical therapy enhances recovery of upper limb function in chronic stroke patients," *Neurorehabil. Neural Repair*, vol. 30, no. 4, pp. 319–348, May 2016, doi: 10.1177/1545968315595285.

[31] H. J. Fassett *et al.*, "Transcranial magnetic stimulation with intermittent theta burst stimulation alters corticospinal output in patients with chronic incomplete spinal cord injury," *Frontiers Neurol.*, vol. 8, p. 380, Aug. 2017, doi: 10.3389/fneur.2017.00380.

[32] M. C. Ridding and J. C. Rothwell, "Is there a future for therapeutic use of transcranial magnetic stimulation?" *Nature Rev. Neurosci.*, vol. 8, no. 7, pp. 559–567, Jul. 2007, doi: 10.1038/nrn2169.

[33] E. G. Lee, P. Rastogi, R. L. Hadimani, D. C. Jiles, and J. A. Camprodon, "Impact of non-brain anatomy and coil orientation on inter- and intra-subject variability in TMS at midline," *Clin. Neurophysiol.*, vol. 129, no. 9, pp. 1873–1883, Sep. 2018, doi: 10.1016/j.clinph.2018.04.749.

[34] M. G. Stokes *et al.*, "Simple metric for scaling motor threshold based on scalp-cortex distance: Application to studies using transcranial magnetic stimulation," *J. Neurophysiol.*, vol. 94, no. 6, pp. 4520–4527, Dec. 2005, doi: 10.1152/JN.00067.2005/ASSET/IMAGES/LARGE/Z9K0120551360003.JPEG.

[35] M. S. Beauchamp *et al.*, "The developmental trajectory of brain-scalp distance from birth through childhood: Implications for functional neuroimaging," *PLoS ONE*, vol. 6, no. 9, Sep. 2011, Art. no. e24981, doi: 10.1371/JOURNAL.PONE.0024981.

[36] F. Syeda, A. Pandurangi, A. A. El-Gendy, and R. L. Hadimani, "Effect of transcranial magnetic stimulation on demyelinated neuron populations," *IEEE Trans. Magn.*, vol. 53, no. 11, pp. 1–4, Nov. 2017, doi: 10.1109/TMAG.2017.2728006.

[37] Z. D. Deng, S. H. Lisanby, and A. V. Peterchev, "Electric field depth-focality tradeoff in transcranial magnetic stimulation: Simulation comparison of 50 coil designs," *Brain Stimulation*, vol. 6, no. 1, pp. 1–13, Jan. 2013, doi: 10.1016/j.brs.2012.02.005.

[38] T. A. Yousry *et al.*, "Localization of the motor hand area to a knob on the precentral gyrus. A new landmark," *Brain*, vol. 120, no. 1, pp. 141–157, 1997, doi: 10.1093/brain/120.1.141.

[39] J. Mak, F. Syeda, and R. L. Hadimani, "3D modeling of diffusion tensor imaging tractography data for finite element analysis," in *Proc. IEEE Int. Symp. Biomed. Imag.*, Apr. 2018, Paper FrP2O-01.11. [Online]. Available: https://embs.papercept.net/conferences/conferences/ISBI18/program/ISBI18_ContentListWeb_3.html

[40] D. Bates, M. Mächler, B. Bolker, and S. Walker, "Fitting linear mixed-effects models using lme4," *J. Stat. Softw.*, vol. 67, no. 1, pp. 1–48, 2015, doi: doi:.10.18637/jss.v067.i01.

[41] *R: The R Project for Statistical Computing*, T. R. Foundation, Vienna, Austria, 2018.

[42] A. Zolj, S. N. Makarov, L. N. de Lara, and A. Nummenmaa, "Electrically small dipole antenna probe for quasistatic electric field measurements in transcranial magnetic stimulation," *IEEE Trans. Magn.*, vol. 55, no. 1, pp. 1–10, Jan. 2019, doi: 10.1109/TMAG.2018.2875882.

[43] A. V. Peterchev *et al.*, "Fundamentals of transcranial electric and magnetic stimulation dose: Definition, selection, and reporting practices," *Brain Stimulation*, vol. 5, no. 4, pp. 435–453, Oct. 2012, doi: 10.1016/j.brs.2011.10.001.

[44] T. Wagner *et al.*, "Transcranial magnetic stimulation and stroke: A computer-based human model study," *NeuroImage*, vol. 30, no. 3, pp. 857–870, Apr. 2006, doi: 10.1016/j.neuroimage.2005.04.046.

[45] S. Rossi, M. Hallett, P. M. Rossini, and A. Pascual-Leone, "Safety, ethical considerations, and application guidelines for the use of transcranial magnetic stimulation in clinical practice and research," *Clin. Neurophys.*, vol. 120, no. 12, pp. 2008–2039, Dec. 2009, doi: 10.1016/j.clinph.2009.08.016.

[46] M. Bortoletto, D. Veniero, G. Thut, and C. Miniussi, "The contribution of TMS–EEG coregistration in the exploration of the human cortical connectome," *Neurosci. Biobehavioral Rev.*, vol. 49, pp. 114–124, Feb. 2015, doi: 10.1016/J.NEUBIOREV.2014.12.014.

[47] R. Li *et al.*, "Cortical hemodynamic response and connectivity modulated by sub-threshold high-frequency repetitive transcranial magnetic stimulation," *Frontiers Hum. Neurosci.*, vol. 13, p. 90, Mar. 2019, doi: 10.3389/FNHUM.2019.00090.

[48] H. Zhang, T. Schneider, C. A. Wheeler-Kingshott, and D. C. Alexander, "NODDI: Practical *in vivo* neurite orientation dispersion and density imaging of the human brain," *NeuroImage*, vol. 61, no. 4, pp. 1000–1016, Jul. 2012, doi: 10.1016/J.NEUROIMAGE.2012.03.072.

[49] E. J. Wallace, J. L. Mathias, L. Ward, J. Fripp, S. Rose, and K. Pannek, "A fixel-based analysis of micro- and macro-structural changes to white matter following adult traumatic brain injury," *Human Brain Mapping*, vol. 41, no. 8, pp. 2187–2197, Jun. 2020, doi: 10.1002/HBM.24939.

[50] (Dec. 2021). Virginia Commonwealth University. *The Effect of Brain Anatomy on the Efficacy of Brain Stimulation Therapy*. Clinicaltrials.gov, Clinical trial registration NCT04586387. [Online]. Available: https://clinicaltrials.gov/ct2/show/NCT04586387